

# Dual Solutions for Stagnation Point Flow of Carbon Nanotube over a Permeable Exponentially Shrinking Sheet and Stability Analysis

Nur Syazana Anuar<sup>1</sup>, Norfifah Bachok<sup>1,2</sup>, Norihan Md Arifin<sup>1,2</sup>, Haliza Rosali<sup>1</sup>

<sup>1</sup>Department of Mathematics, Faculty of Science, Universiti Putra Malaysia, 43400 UPM Serdang, Selangor, Malaysia

<sup>2</sup>Institute for Mathematical Research, Universiti Putra Malaysia, 43400 UPM Serdang, Selangor, Malaysia

**Abstract**—The stagnation point flow of carbon nanotube (CNT) over an exponentially shrinking sheet in the presence of suction/injection effects is investigated. Two kinds of CNT are used as nanoparticles i.e. single wall carbon nanotube and multi wall carbon nanotube. The partial differential equations are reduced to a set of nonlinear ordinary differential equations using a similarity transformation and it is solved numerically using the function *bvp4c* from Matlab for different values of the governing parameters. Numerical results for the skin friction coefficient and local Nusselt number as well as velocity and temperature profiles are obtained and illustrated graphically. It is found that the similarity equations have two solutions, first and second solutions, in a certain range of shrinking parameters. The suction parameter delays the boundary layer separation, meanwhile injection accelerates it. Results also show that single wall carbon nanotube provides higher skin friction and heat transfer compared to multi wall carbon nanotube. In order to determine the stability of the solutions, stability analysis is performed. Hence, it is found that the first solution is stable and the second solution is unstable.

**Keywords**—carbon nanotube; dual solutions; exponentially shrinking; stability analysis; suction/injection.

## NOMENCLATURE

$a, b$	constant
$C_f$	skin friction coefficient
$C_p$	specific heat at constant temperature
$f$	dimensionless stream function
$k$	thermal conductivity
$L$	characteristic length of a sheet
$Nu_x$	local Nusselt number
$Pr$	Prandtl number
$q_w$	surface heat flux
$Re_x$	local Reynolds number
$s$	suction/injection

$t$	time
$T$	temperature
$T_o$	constant
$u, v$	velocity components along the $x$ - and $y$ - directions, respectively
$U_w$	stretching/shrinking velocity
$U_\infty$	velocity of inviscid flow
$x, y$	cartesian coordinates along the surface and normal to it, respectively

## Greek symbols

$\alpha$	thermal diffusivity
$\phi$	nanoparticle volume fraction
$\theta$	dimensionless temperature
$\gamma$	unknown eigenvalues
$\varepsilon$	shrinking parameter
$\nu$	kinematic viscosity
$\mu$	dynamic viscosity
$\rho$	fluid density
$\rho C_p$	heat capacity of the fluid
$\tau$	dimensionless time variable
$\tau_w$	surface shear stress
$\psi$	stream function
$\eta$	similarity variable

## Subscripts

$w$	condition at the surface of the plate
$\infty$	ambient condition
$CNT$	carbon nanotubes
$f$	fluid
$nf$	nanofluid

## I. INTRODUCTION

Carbon nanotube was first introduced in 1991 by Iijima [1] and it is classified into two kinds of carbon nanotubes such as single wall carbon nanotube (SWCNT) and multi wall carbon nanotube (MWCNT). The thermal conductivity of carbon nanotubes is found to improve significantly compared to pure fluids and therefore there is an increasing interest in the

applications of single wall and multi wall carbon nanotube in industry, technologies and medical fields [2,3,4]. Meanwhile, important work on boundary layer flow of carbon nanotube has been reported by Khan et al. [5] using a Xue's model [6]. Hayat et al. [7] conducted similar research on carbon nanotube over stretching cylinder using homotopy analysis method. The effect of slip on boundary layer flow of moving surface along with stability analysis was discussed by Anuar et al. [8]. Recently, Anuar et al. [9] investigated stagnation point flow over an exponentially stretching/shrinking sheet with homogeneous-heterogeneous reaction effect. Several other authors have investigated the boundary layer flow of carbon nanotube in their research [10,11,12].

Nowadays, the investigation of boundary layer flow and heat transfer over a stretching/shrinking sheet has gain a lot of interest due to its outstanding significance in manufacturing and engineering processes. The characteristics of heat and mass transfer on boundary layer flow due to an exponentially continuous stretching sheet have been examined numerically by Magyari and Keller [13]. Afterwards, Elbashbeshy [14] studied the heat transfer phenomena over an exponentially stretching continuous surface with the effect of suction. The problem of exponentially shrinking sheet was made by Bhattacharyya [15]. A year later, Bhattacharyya and Vajravelu [16] studied similar research near the stagnation region. They obtained dual solutions as well as unique solution for certain values of stretching and shrinking parameter. Some very important investigations on boundary layer flow over an exponentially stretching/shrinking sheet can also be found in the articles [17,18,19].

Majority of the researchers obtained more than one solution for a certain parameter in their studies. It seems that the idea to identify the stability of the solutions obtained has been proposed by Merkin [20]. This analysis later was continued by Weidman et al. [21], Merrill et al. [22], Harris et al. [23], Ishak [24], Dzulkifli et al. [25], Bakar et al. [26] and many more. They concluded that the first solution is stable solution meanwhile the second solution is unstable solution.

Motivated by the above works, we have attempted here to extend the paper by Bhattacharyya and Vajravelu [16] to the case where the plate is permeable and considered in carbon nanotubes, together with stability analysis [9]. Two kinds of carbon nanotubes are considered such as single wall carbon nanotube (SWCNT) and multi wall carbon nanotube (MWCNT) with water as the base fluid.

## II. MATHEMATICAL FORMULATION

We consider the steady two-dimensional boundary layer flow near the stagnation point on a semi-infinite permeable exponentially shrinking surface in carbon nanotubes, where  $x$  and  $y$  are Cartesian coordinate measured along the shrinking surface and normal to it. A schematic representation of physical model and coordinate system are shown in Figure 1. Moreover,

the flow is confined at  $y > 0$ . Single wall (SWCNT) and multi wall (MWCNT) carbon nanotubes are treated as nanoparticle with water as the based fluid. It is assumed that the shrinking velocity  $U_w(x) = ae^{x/L}$ , ambient fluid velocity  $U_\infty(x) = be^{x/L}$  and surface temperature  $T_w(x) = T_\infty + T_o e^{2x/L}$  vary exponentially, where  $a, b$  and  $T_o$  are constants,  $T_\infty$  is the temperature far away from the shrinking sheet and  $L$  is the reference length. Under the boundary layer approximation, the governing boundary layer equations are written as [16,9]

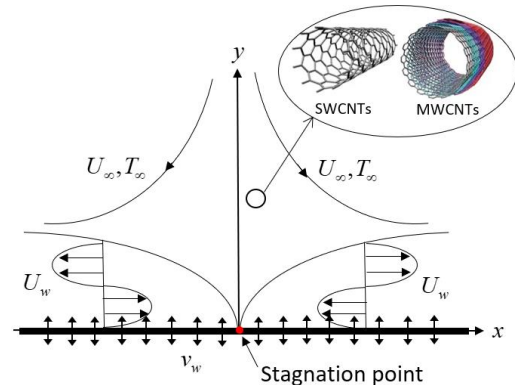


Fig. 1. Physical model for shrinking sheet

$$\frac{\partial u}{\partial x} + \frac{\partial v}{\partial y} = 0, \quad (1)$$

$$u \frac{\partial u}{\partial x} + v \frac{\partial u}{\partial y} = U_\infty \frac{dU_\infty}{dx} + \frac{\mu_{nf}}{\rho_{nf}} \frac{\partial^2 u}{\partial y^2}, \quad (2)$$

$$u \frac{\partial T}{\partial x} + v \frac{\partial T}{\partial y} = \alpha_{nf} \frac{\partial^2 T}{\partial y^2}, \quad (3)$$

with the boundary conditions

$$\begin{aligned} u = U_w(x), \quad v = v_w(x), \quad T = T_w(x) \quad \text{at } y = 0, \\ u \rightarrow U_\infty(x), \quad T \rightarrow T_\infty \quad \text{as } y \rightarrow \infty, \end{aligned} \quad (4)$$

where  $u$  and  $v$  are the velocity components in the  $x$  and  $y$  direction, respectively. It should be mention that  $v_w(x) = -(v_f b / 2L)^{1/2} e^{x/2L} s$ , where  $s > 0$  represent suction,  $s < 0$  for injection and  $s = 0$  for impermeable surface. Additionally,  $\mu_{nf}$ ,  $\rho_{nf}$  and  $\alpha_{nf}$  is the viscosity, density and thermal diffusivity of nanofluid which are defined as [27,6]

$$\alpha_{nf} = \frac{k_{nf}}{(\rho C_p)_{nf}}, \quad \mu_{nf} = \frac{\mu_f}{(1-\phi)^{2.5}},$$

$$\rho_{nf} = (1-\phi)\rho_f + \phi\rho_{CNT},$$

$$(\rho C_p)_{nf} = (1-\phi)(\rho C_p)_f + \phi(\rho C_p)_{CNT}, \quad (5)$$

$$\frac{k_{nf}}{k_f} = \frac{1-\phi + 2\phi \frac{k_{CNT}}{k_{CNT}-k_f} \ln \frac{k_{CNT}+k_f}{2k_f}}{1-\phi + 2\phi \frac{k_f}{k_{CNT}-k_f} \ln \frac{k_{CNT}+k_f}{2k_f}},$$

where  $\phi$  is the nanoparticle volume fraction,  $\mu_f$  is the viscosity of the base fluid,  $(\rho C_p)_{nf}$  is the effective heat capacity of a nanoparticle,  $(\rho C_p)_f$  and  $(\rho C_p)_{CNT}$  are the effective heat capacities of the base fluid and carbon nanotubes, respectively,  $k_{nf}$  is the thermal conductivity of nanofluid,  $k_f$  and  $k_{CNT}$  are the thermal conductivities of base fluid and carbon nanotubes, respectively,  $\rho_f$  and  $\rho_{CNT}$  are the density of the base fluid and carbon nanotubes, respectively.

We introduced now the following appropriate similarity transformation:

$$\eta = y \left( \frac{b}{2\nu_f L} \right)^{1/2} e^{x/2L}, \quad \psi = (2\nu_f L b)^{1/2} f(\eta) e^{x/2L},$$

$$\theta(\eta) = \frac{T - T_\infty}{T_w - T_\infty}, \quad (6)$$

where  $\eta$  is the similarity variable,  $\nu_f$  is the kinematic viscosity and  $\psi$  is the stream function which defined as  $u = \partial\psi/\partial y$  and  $v = -\partial\psi/\partial x$  where identically satisfies equation (1).

Inserting equation (6) into equations (2) – (4), yields the following nonlinear ordinary differential equations

$$\frac{1}{(1-\phi)^{2.5} (1-\phi + \phi\rho_{CNT}/\rho_f)} f''' + ff'' - 2f'^2 + 2 = 0, \quad (7)$$

$$\frac{1}{Pr \left[ 1 - \phi + \phi(\rho C_p)_{CNT}/(\rho C_p)_f \right]} \theta'' + f\theta' - f'\theta = 0, \quad (8)$$

and the transformed boundary conditions are

$$f(0) = s, \quad f'(0) = \varepsilon, \quad \theta(0) = 1,$$

$$f'(\eta) \rightarrow 1, \quad \theta(\eta) \rightarrow 0 \quad \text{as } \eta \rightarrow \infty. \quad (9)$$

Here, prime denotes differentiation with respect to  $\eta$ ,  $Pr = \nu_f/\alpha_f$  is the Prandtl number and  $\varepsilon = a/b$  is the shrinking sheet.

The quantities of physical interest are the local skin friction  $C_f$  and local Nusselt number  $Nu_x$  that are defined as

$$C_f = \frac{\tau_w}{\rho_f U_w^2}, \quad Nu_x = \frac{2Lq_w}{k_f (T_w - T_\infty)}, \quad (10)$$

where  $\tau_w$  is the shear stress and  $q_w$  is the heat flux at the surface that given by

$$\tau_w = \mu_{nf} \left( \frac{\partial u}{\partial y} \right)_{y=0}, \quad q_w = -k_{nf} \left( \frac{\partial T}{\partial y} \right)_{y=0}. \quad (11)$$

Substituting equation (11) into equation (10) and using variable (6), we obtain

$$C_f Re_x^{1/2} = \frac{f''(0)}{(1-\phi)^{2.5}}, \quad Nu_x Re_x^{-1/2} = -\frac{k_{nf}}{k_f} \theta'(0), \quad (12)$$

where  $Re_x = 2La/\nu_f$  is the local Reynolds number.

### III. FLOW STABILITY

The obtained results show the existence of dual solutions, therefore it is important to find the physical reliability of these solutions. In this respect, we need to consider the problem in unsteady case. The new variable  $\tau$  that is associated with the initial value problem are introduced [20,21]. So, equations (2) – (4) are rewrite as follows:

$$\frac{\partial u}{\partial t} + u \frac{\partial u}{\partial x} + v \frac{\partial u}{\partial y} = U_\infty \frac{dU_\infty}{dx} + \frac{\mu_{nf}}{\rho_{nf}} \frac{\partial^2 u}{\partial y^2}, \quad (13)$$

$$\frac{\partial T}{\partial t} + u \frac{\partial T}{\partial x} + v \frac{\partial T}{\partial y} = \alpha_{nf} \frac{\partial^2 T}{\partial y^2}, \quad (14)$$

subject to boundary conditions

$$u = U_w(x), \quad v = v(x), \quad T = T_w(x) \quad \text{at } y = 0,$$

$$u \rightarrow U_\infty(x), \quad T \rightarrow T_\infty \quad \text{as } y \rightarrow \infty, \quad (15)$$

where  $t$  represents time. As identified by variable (6), we introduced the new dimensionless variable for the unsteady problem

$$\eta = y \left( \frac{b}{2\nu_f L} \right)^{1/2} e^{x/2L}, \quad \psi = (2\nu_f L b)^{1/2} f(\eta, \tau) e^{x/2L},$$

$$\theta(\eta, \tau) = \frac{T - T_\infty}{T_w - T_\infty}, \quad \tau = \frac{bt}{2L} e^{x/2L}, \quad (16)$$

thus equations (13) – (15) can be written as

$$\frac{1}{(1-\phi)^{2.5} (1-\phi + \phi\rho_{CNT}/\rho_f)} \frac{\partial^3 f}{\partial \eta^3} - 2 \left( \frac{\partial f}{\partial \eta} \right)^2 + 2$$

$$+ f \frac{\partial^2 f}{\partial \eta^2} - 2\tau \left( \frac{\partial f}{\partial \eta} \frac{\partial^2 f}{\partial \eta \partial \tau} - \frac{\partial f}{\partial \tau} \frac{\partial^2 f}{\partial \eta^2} \right) - \frac{\partial^2 f}{\partial \eta \partial \tau} = 0, \quad (17)$$

$$\frac{1}{Pr \left[ 1 - \phi + \phi(\rho C_p)_{CNT}/(\rho C_p)_f \right]} \frac{\partial^2 \theta}{\partial \eta^2} + f \frac{\partial \theta}{\partial \eta}$$

$$- \theta \frac{\partial f}{\partial \eta} - 2\tau \left( \frac{\partial f}{\partial \eta} \frac{\partial \theta}{\partial \tau} - \frac{\partial f}{\partial \tau} \frac{\partial \theta}{\partial \eta} \right) - \frac{\partial \theta}{\partial \tau} = 0, \quad (18)$$

subject to the boundary conditions

$$f(0, \tau) = s, \quad \frac{\partial f}{\partial \eta}(0, \tau) = \varepsilon, \quad \theta(0, \tau) = 1, \quad (19)$$

$$\frac{\partial f}{\partial \eta}(\eta, \tau) \rightarrow 1, \quad \theta(\eta, \tau) \rightarrow 0 \quad \text{as } \eta \rightarrow \infty.$$

To identify the stability solution  $f(\eta) = f_o(\eta)$  and  $\theta(\eta) = \theta_o(\eta)$  fulfilling the boundary-value problem, we introduced the following term (see [21]):

$$f(\eta, \tau) = f_o(\eta) + e^{-\gamma\tau} F(\eta, \tau), \quad (20)$$

$$\theta(\eta, \tau) = \theta_o(\eta) + e^{-\gamma\tau} H(\eta, \tau),$$

where  $\gamma$  is an unknown eigenvalue,  $F(\eta)$  and  $H(\eta)$  are small relative to  $f_o(\eta)$  and  $\theta_o(\eta)$ . Using equation (20) into equations (17) – (19), followed by setting  $\tau = 0$  and hence substituting  $F = F_o(\eta)$  and  $H = H_o(\eta)$ , the linearized problem is given by

$$\frac{1}{(1-\phi)^{2.5} (1-\phi + \phi \rho_{CNT} / \rho_f)} F_o''' + f_o F_o'' + f_o'' F_o - (4f_o' - \gamma) F_o' = 0, \quad (21)$$

$$\frac{1}{\text{Pr} \left[ 1 - \phi + \phi (\rho C_p)_{CNT} / (\rho C_p)_f \right]} H_o'' + f_o H_o' + F_o \theta_o' - F_o' \theta_o - H_o f_o' + \gamma H_o = 0, \quad (22)$$

along with boundary conditions

$$F_o(0) = 0, \quad F_o'(0) = 0, \quad H_o(0) = 0, \quad (23)$$

$$F_o'(\eta) \rightarrow 0, \quad H_o(\eta) \rightarrow 0, \quad \text{as } \eta \rightarrow \infty.$$

To find the possible eigenvalues, we relax  $F_o'(0) \rightarrow 0$  as  $\eta \rightarrow \infty$  (see [23]). Therefore, the system of equations (21) – (23) along with the new boundary condition  $F_o''(0) = 1$  need to be solved.

#### IV. RESULTS AND DISCUSSION

The transformed system of uncoupled nonlinear ordinary differential equations (7) and (8) with the boundary conditions (9) was solved numerically using the bvp4c solver for various parameter values such as suction/injection and carbon nanotubes in Matlab software. The impacts of the evolving parameters on the dimensionless velocity, temperature, skin friction coefficient and local Nusselt number are analyzed and numerically investigated. The thermophysical properties of the base fluid (water) and the nanoparticles are taken from Table I. The range of nanoparticle volume fraction  $\phi$  are taken from 0 to 0.2 and Prandtl number is 6.2 ( $\text{Pr} = 6.2$ ). Figures 2 and 3 show the variation of reduced skin friction  $f''(0)$  and heat transfer  $-\theta'(0)$  with shrinking parameter  $\varepsilon$  for

various value of suction/injection. It is observed that the value of  $|\varepsilon_c|$  increase as  $s$  increases. Hence, we can conclude that introducing suction ( $s > 0$ ) is to increase the range of solution and consequently delay the boundary layer separation, while injection ( $s < 0$ ) accelerates the boundary layer separation. The suction effect is seen to increase the skin friction and heat transfer rate at the surface, while the reverse pattern happens for the effect of injection.

Figures 4 – 7 represent the variation of reduced skin friction  $f''(0)$  and heat transfer  $-\theta'(0)$  for different carbon nanotube with the existence of suction ( $s = 0.3$ ) and injection ( $s = -0.3$ ). It is shown that single wall carbon nanotube (SWCNT) offers a higher skin friction and heat transfer rate compared to multi wall carbon nanotube (MWCNT) for both suction and injection case. Furthermore, for the suction case, the range of  $\varepsilon$ , where solution exists is increased for SWCNT and it decreased for MWCNT; whereas for the case of injection, the range of solution exist is entirely opposite for SWCNT and MWCNT. It is worth noting that Figures 2 – 7 show the region of unique solution exists for  $\varepsilon > -1$  and the solution is non-unique for  $\varepsilon_c \leq \varepsilon \leq -1$  whereby no solution exists beyond this critical point, i.e. there is boundary layer separation when  $\varepsilon < \varepsilon_c$ .

Figures 8 and 9 demonstrate the variation of skin friction coefficient  $C_f \text{Re}_x^{1/2}$  and local Nusselt number  $Nu_x \text{Re}_x^{-1/2}$  with nanoparticle volume fraction  $\phi$  for different suction/injection parameter  $s$  and carbon nanotubes. It is observed that suction/injection parameter and carbon nanotubes grow monotonically as nanoparticle volume fraction increases. It is further evidenced from these figures that suction surface ( $s = 0.3$ ) offers higher skin friction coefficient and local Nusselt number compared to injection surface ( $s = -0.3$ ) and impermeable surface ( $s = 0$ ). In addition, skin friction coefficient and local Nusselt number is found to be highest for SWCNT compared to MWCNT.

The velocity  $f'(\eta)$  and temperature  $\theta(\eta)$  profile for several values of suction/injection parameter  $s$  are plotted in Figures 10 and 11. It is noted that the thickness of the boundary layer for second solution is greater than the first solution. These profiles support the existence of dual nature of solutions as shown in Figures 2 – 7. It is also observed that the value of the fluid velocity increases with increasing suction for the first solution and the velocity decreases with increasing suction in the second solution. Meanwhile, in the temperature profile, the reverse behaviors are noted for both solutions

In order to perform stability analysis, the system of linearized problems (21) and (22) with the boundary conditions (23) have been applied into bvp4c solver in Matlab software. The stability of the solutions is tested

by finding a smallest eigenvalue  $\gamma$ . If the obtained smallest eigenvalues are positive, the solution is stable, meanwhile if the smallest eigenvalues are negative, it is unstable solution. Table II represents the smallest eigenvalues for selected values of suction/injection parameter  $s$  and shrinking parameter  $\varepsilon$ . The first solutions are seen to have positive smallest eigenvalue while the second solutions have negative smallest eigenvalue. We can therefore conclude that the first solution is stable while the second solution is unstable. On the other hand, it is clearly seen from Table II that as the value of shrinking parameter approaches to its critical value  $\varepsilon_c$ , the eigenvalue  $\gamma$  will approaching zero ( $\gamma \rightarrow 0$ ).

TABLE I. THERMOPHYSICAL PROPERTIES OF CNTs [5]

Physical properties	Base fluid (water)	Nanoparticle	
		SWCNT	MWCNT
$\rho(kg/m^3)$	997	2600	1600
$C_p(J/kgK)$	4179	425	796
$k(W/mK)$	0.613	6600	3000

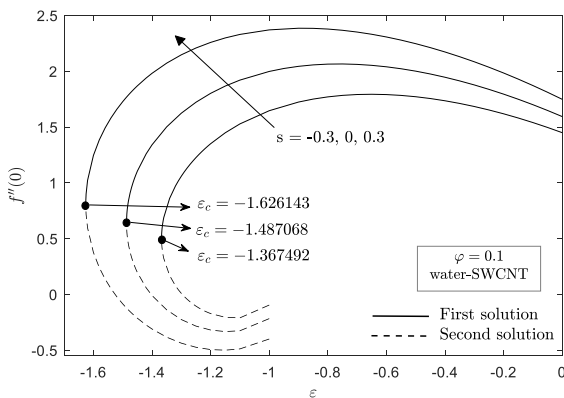


Fig. 2. Variation of  $f''(0)$  with  $\varepsilon$  for different value of suction

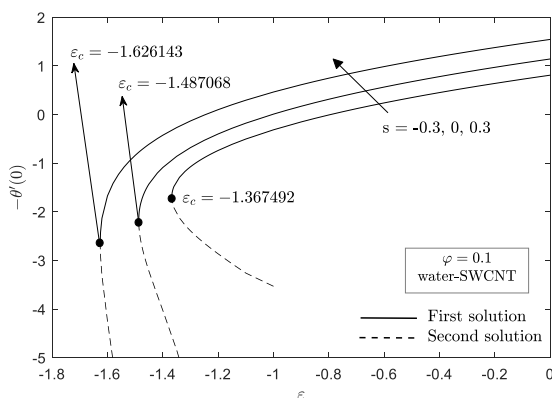


Fig. 3. Variation of  $-\theta'(0)$  with  $\varepsilon$  for different value of suction

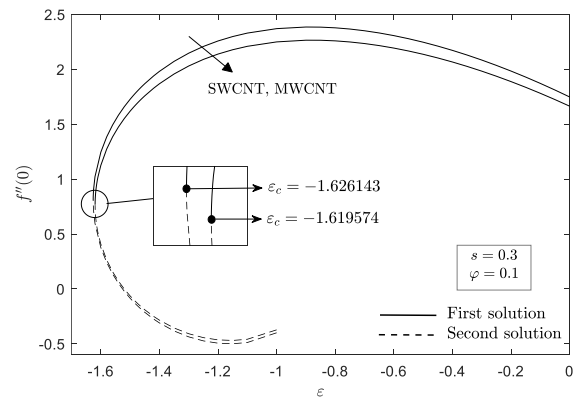


Fig. 4. Variation of  $f''(0)$  with  $\varepsilon$  for different carbon nanotubes when  $s = 0.3$

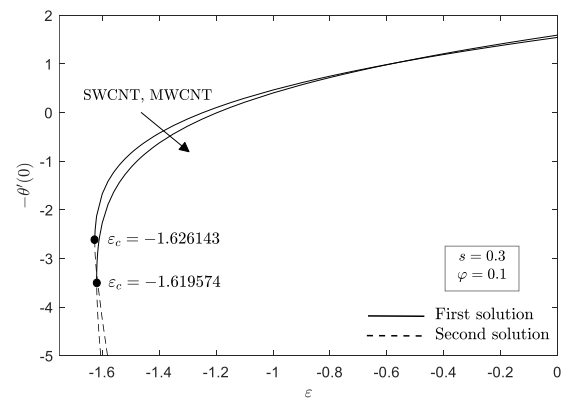


Fig. 5. Variation of  $-\theta'(0)$  with  $\varepsilon$  for different carbon nanotubes when  $s = 0.3$

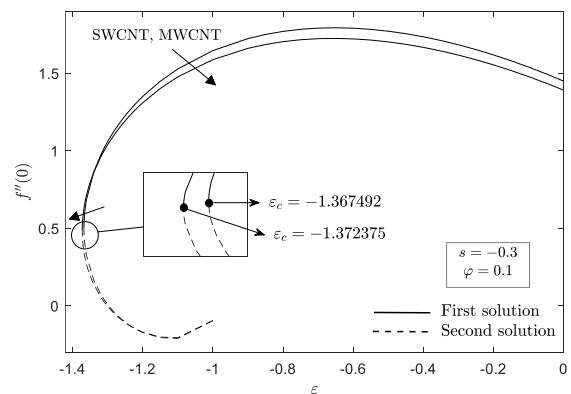


Fig. 6. Variation of  $f''(0)$  with  $\varepsilon$  for different carbon nanotubes when  $s = -0.3$

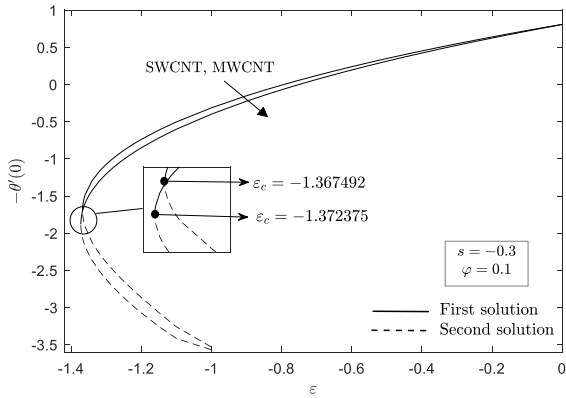


Fig. 7. Variation of  $-\theta'(0)$  with  $\varepsilon$  for different carbon nanotubes when  $s = -0.3$

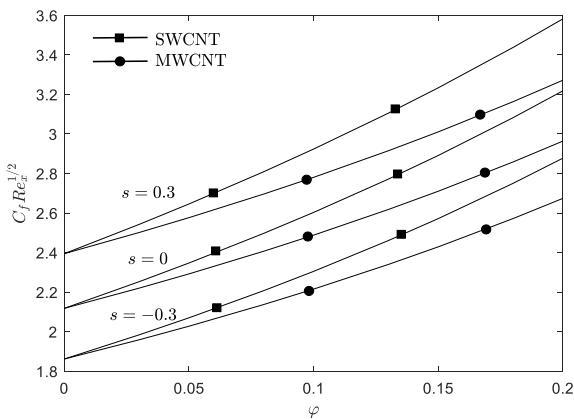


Fig. 8. Variation of  $C_f Re_x^{1/2}$  with  $\phi$  for different carbon nanotubes and suction

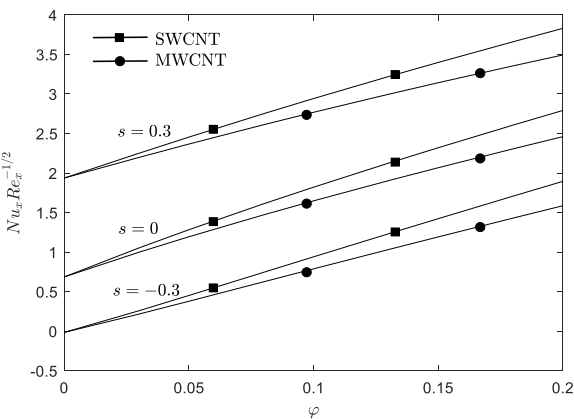


Fig. 9. Variation of  $Nu_x Re_x^{-1/2}$  with  $\phi$  for different carbon nanotubes and suction

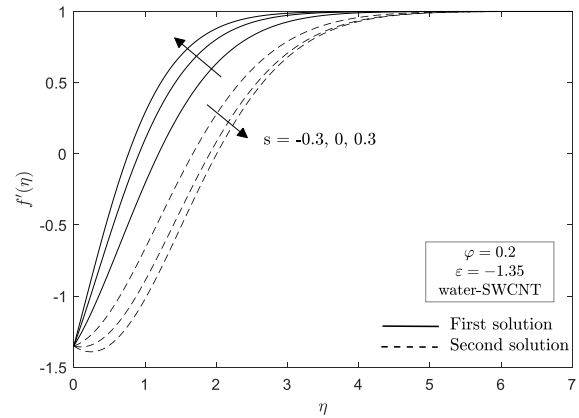


Fig. 10. Velocity profile for different values of suction

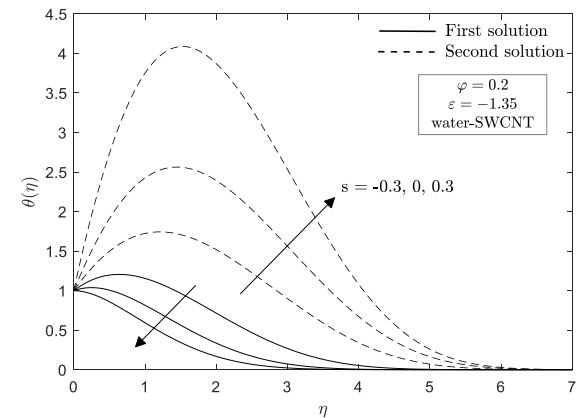


Fig. 11. Temperature profile for different values of suction

TABLE II. SMALLEST EIGENVALUES OF  $\gamma$  FOR DIFFERENT VALUES OF  $s$  AND  $\varepsilon$  WHEN  $\phi = 0.1$  (WATER-SWCNT)

$s$	$\varepsilon$	First solution	Second solution
-0.3	-1.36749	0.0055	-0.0055
	-1.367	0.1110	-0.1107
	-1.36	0.4341	-0.4307
0	-1.48706	0.0147	-0.0147
	-1.487	0.0413	-0.0413
	-1.48	0.4202	-0.4168
0.3	-1.62614	0.0073	-0.0073
	-1.626	0.0595	-0.0595
	-1.62	0.3919	-0.3889

## V. CONCLUSIONS

The problem of the stagnation point flow over an exponentially shrinking sheet in carbon nanotubes with suction effect has been studied in this paper. The governing ordinary differential equations were solved numerically using the bvp4c solver from Matlab. For several values of the governing parameters, the numerical results obtained for the velocity and

temperature profiles as well as the skin friction coefficient and local Nusselt number are shown graphically. It was found that dual solutions exist for a certain range of shrinking parameter. It was also shown that suction delays the boundary layer separation, while injection accelerates it. The highest values of the skin friction coefficient and the local Nusselt number were obtained for the single wall carbon nanotube compared to multi wall carbon nanotube. Additionally, the skin friction coefficients and local Nusselt number are found to increase for suction parameter and to decrease for injection parameter. A stability analysis was carried out to determine the stability of the dual solutions obtained, and it was concluded that the first solution was stable and physically feasible, while the second solution was unstable.

#### ACKNOWLEDGMENT

This study was supported by Fundamental Research Grant Scheme (FRGS/1/2018/STG06/UPM/02/4/5540155) and MyBrainSc from the Ministry of Higher Education, Malaysia.

#### REFERENCES

- [1] S. Iijima, "Helical microtubules of graphitic carbon," *Nature*, vol. 354, no. 6348, pp. 56–58, Nov. 1991.
- [2] R.H. Baughman, A.A. Zakhidov, W.A. De Heer, "Carbon nanotubes--the route toward applications," *science*, vol. 297, no. 5582, pp. 787-792, Sep. 2002.
- [3] A. Bianco, K. Kostarelos, M. Prato, "Applications of carbon nanotubes in drug delivery," *Current opinion in chemical biology*, vol. 9, no. 6, pp. 674-679. Oct. 2005.
- [4] M.F. De Volder, S.H. Tawfick, R.H. Baughman, A.J. Hart, "Carbon nanotubes: present and future commercial applications," *science*, vol. 339, no. 6119, pp. 535-539, Feb. 2013.
- [5] W.A. Khan, Z.H. Khan, M. Rahi, "Fluid flow and heat transfer of carbon nanotubes along a flat plate with Navier slip boundary," *Applied Nanoscience*, vol. 4, no. 5, pp. 633-641, June 2014.
- [6] Q.Z. Xue, "Model for thermal conductivity of carbon nanotube-based composites," *Physica B: Condensed Matter*, vol. 368, no. 1-4, pp. 302-307. Nov. 2005.
- [7] T. Hayat, M. Farooq, A. Alsaedi, "Stagnation point flow of carbon nanotubes over stretching cylinder with slip conditions," *Open Physics*, vol. 13, no. 1, Jan. 2015.
- [8] N.S. Anuar, N. Bachok, I. Pop, "A Stability Analysis of Solutions in Boundary Layer Flow and Heat Transfer of Carbon Nanotubes over a Moving Plate with Slip Effect," *Energies*, vol. 11, no. 12, pp. 3243, Nov. 2018.
- [9] N.S. Anuar, N. Bachok, N.M. Arifin, H. Rosali, "Stagnation Point Flow and Heat Transfer over an Exponentially Stretching/Shrinking Sheet in CNT with Homogeneous–Heterogeneous Reaction: Stability Analysis," *Symmetry*, vol. 11, no. 4, pp. 522. April 2019.
- [10] M. Jawad, Z. Shah, S. Islam, J. Majdoubi, I. Tlili, W. Khan, I. Khan, "Impact of nonlinear thermal radiation and the viscous dissipation effect on the unsteady three-dimensional rotating flow of single-wall carbon nanotubes with aqueous suspensions," *Symmetry*, vol. 11, no.2, pp. 207. Feb. 2019.
- [11] Y. Reddy, M.S. Reddy, "Heat and Mass Transfer Analysis of Single Walled Carbon Nanotubes and Multi Walled Carbon Nanotubes-Water Nanofluid Flow Over Porous Inclined Plate with Heat Generation/Absorption," *Journal of Nanofluids*, vol. 8, no. 5, pp. 1147-1157. May 2019.
- [12] T. Hayat, K. Muhammad, M.I. Khan, A. Alsaedi, "Theoretical investigation of chemically reactive flow of water-based carbon nanotubes (single-walled and multiple walled) with melting heat transfer," *Pramana*, vol. 92, no. 4, pp. 57, April 2019.
- [13] E. Magyari, B. Keller, "Heat and mass transfer in the boundary layers on an exponentially stretching continuous surface," *Journal of Physics D: Applied Physics*, vol. 32, no. 5, pp. 577–585, 1999.
- [14] E.M.A Elbashbeshy, "Heat transfer over an exponentially stretching continuous surface with suction," *Archives of Mechanics*, vol. 53, no. 6, pp. 643-651, May 2001.
- [15] K. Bhattacharyya, "Boundary layer flow and heat transfer over an exponentially shrinking sheet," *Chinese Physics Letters*, vol. 28, no. 7, pp. 074701, April 2011.
- [16] K. Bhattacharyya, K. Vajravelu, "Stagnation-point flow and heat transfer over an exponentially shrinking sheet," *Communications in Nonlinear Science and Numerical Simulation*, vol. 17, no. 7, pp. 2728-2734, July 2012.
- [17] S. Ghosh, S. Mukhopadhyay, "Flow and heat transfer of nanofluid over an exponentially shrinking porous sheet with heat and mass fluxes," *Propulsion and Power Research*, vol. 7, no. 3, pp. 268-275, Sept. 2018.
- [18] N.L. Aleng, N. Bachok, "Dual solutions of exponentially stretched/shrunk flows of nanofluids," *Journal of Nanofluids*, vol. 7, no. 1, pp. 195-202, Feb. 2018.
- [19] U. Farooq, D. Lu, S. Munir, M. Ramzan, M. Suleman, S. Hussain, S. "MHD flow of Maxwell fluid with nanomaterials due to an exponentially stretching surface," *Scientific reports*, vol. 9, no. 1, pp. 7312, May 2019.

[20] J. Merkin, "On dual solutions occurring in mixed convection in a porous medium," *Journal of Engineering Mathematics*, vol. 20, no. 2, pp 171-179, June 1986.

[21] P. Weidman, D. Kubitschek, A. Davis, "The effect of transpiration on self-similar boundary layer flow over moving surfaces," *International Journal of Engineering Science*, vol. 44, no. 11, pp. 730–7, July 2006.

[22] K. Merrill, M. Beauchesne, J. Previte, J. Paultet, P. Weidman, "Final steady flow near a stagnation point on a vertical surface in a porous medium," *International Journal of Heat and Mass Transfer*, vol. 49, pp. 4681–4686, Nov. 2006.

[23] S.D. Harris, D.B. Ingham, I. Pop, "Mixed convection boundary-layer flow near the stagnation point on a vertical surface in a porous medium: Brinkman model with slip," *Transport in Porous Media*, vol. 77, no. 2, pp. 267–285, March 2009.

[24] A. Ishak, "Flow and heat transfer over a shrinking sheet: A stability Analysis," *International Journal of Mechanical, Aerospace, Industrial and Mechatronics Engineering*, vol. 8, no. 5, pp. 902, 2014.

[25] N.F. Dzulkipli, N. Bachok, I. Pop, N.A. Yacob, N.M. Arifin, H. Rosali, "Soret and Dufour effects on unsteady boundary layer flow and heat transfer of nanofluid over a stretching/shrinking sheet: A stability analysis," *Journal of Chemical Engineering & Process Technology*, vol. 8, no. 3, pp. 1000336, Jan. 2017.

[26] N.A.A. Bakar, N. Bachok, N.M. Arifin, "Stability analysis on the flow and heat transfer of nanofluid past a stretching/shrinking cylinder with suction effect," *Results in Physics*, vol. 9, pp. 1335-1344, June 2018.

[27] H.F. Oztop, E. Abu-Nada, "Numerical study of natural convection in partially heated rectangular enclosures filled with nanofluids," *International Journal of Heat and Fluid Flow*, vol. 29, no. 5, pp. 1326-1336, Oct. 2008.